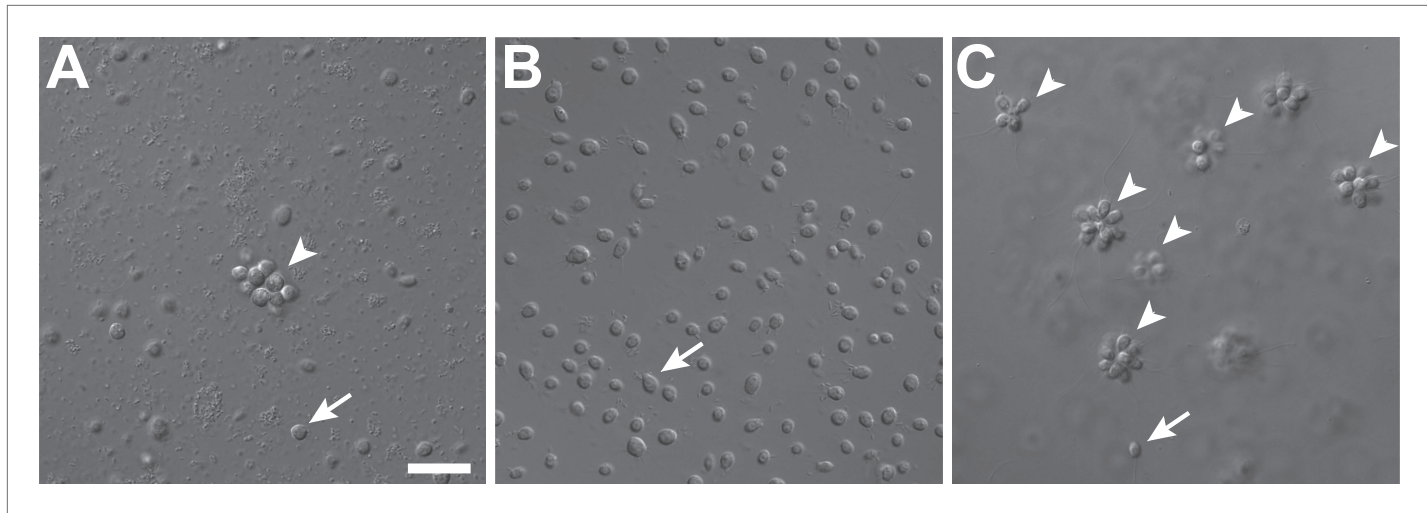


---

## Figures and figure supplements

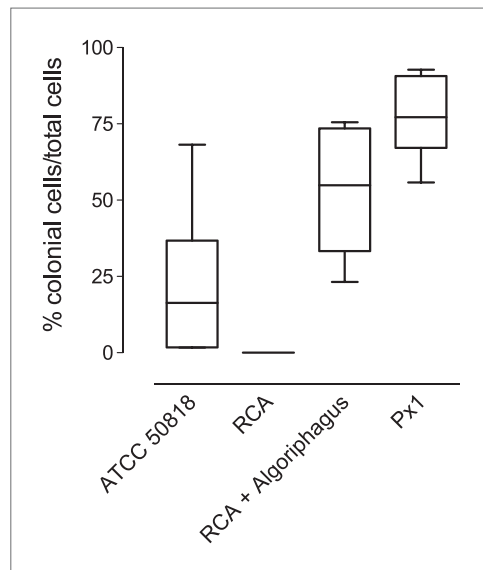
A bacterial sulfonolipid triggers multicellular development in the closest living relatives of animals

**Rosanna A Alegado, et al.**



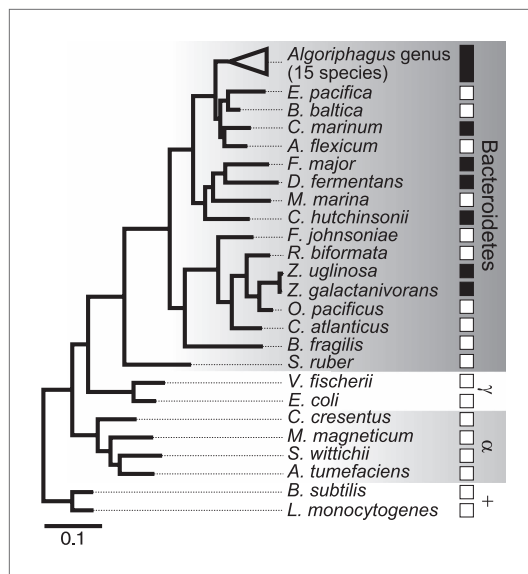
**Figure 1.** Rosette colony development in *S. rosetta* is regulated by *A. machiponganensis*. (A) The original culture of *S. rosetta*, ATCC 50818, contains diverse co-isolated environmental bacteria and forms rosette colonies (arrowheads) rarely. (B) Treatment of ATCC50818 with a cocktail of antibiotics reduced the bacterial diversity and yielded an *S. rosetta* culture line, RCA, in which rosette colonies never formed. (Representative single cells indicated by arrows.) (C) Addition of *A. machiponganensis* to RCA cultures was sufficient to induce rosette development. Scale bar, 2  $\mu$ m.

DOI: 10.7554/eLife.00013.003



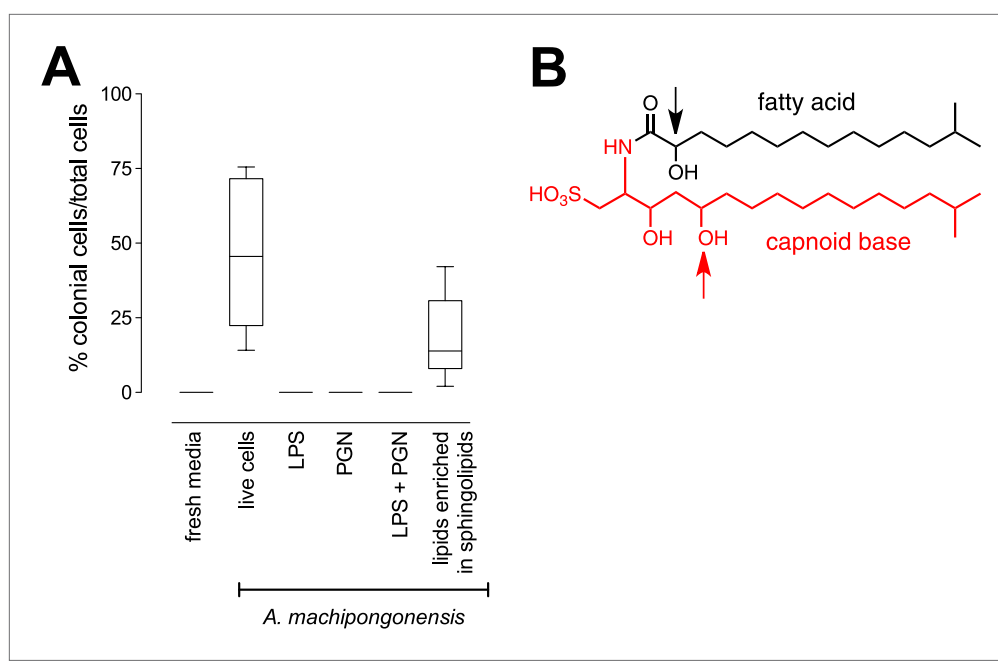
**Figure 1—figure supplement 1.** Frequency of rosette colonies in *S. rosetta* environmental isolate ATCC 50818, RCA with and without *A. machiponganensis* and a monoxenic line with *A. machiponganensis* feeder bacteria (Px1). Altering bacterial diversity in *S. rosetta* cultures alters the frequency of rosette colonies. Data are the whisker-box plots of the frequency of colonial cells in ATCC 50818 and a monoxenic culture of *S. rosetta* fed only *A. machiponganensis* bacteria (Px1) for three experiments.

DOI: 10.7554/eLife.00013.004



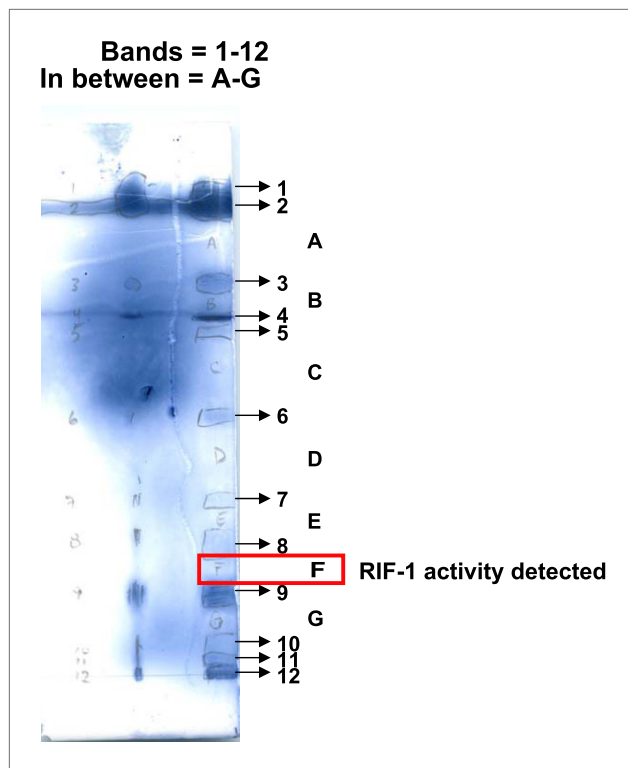
**Figure 2.** Diverse members of the Bacteroidetes phylum induce rosette colony development. A maximum likelihood phylogeny inferred from 16S rDNA gene sequences reveals the evolutionary relationships among *A. machipongonensis*, other members of the Bacteroidetes phylum, and representative  $\gamma$ -proteobacteria ( $\gamma$ ),  $\alpha$ -proteobacteria ( $\alpha$ ), and Gram-positive (+) bacteria. All 15 members of the *Algoriphagus* genus (Table 1), as well as six other species in the Bacteroidetes phylum, were competent to induce colony development (filled squares). In contrast, no species outside of Bacteroidetes and most of the non-*Algoriphagus* bacteria tested failed to induce rosette colony development (open squares). Scale bar, 0.1 substitutions per nucleotide position.

DOI: 10.7554/eLife.00013.006



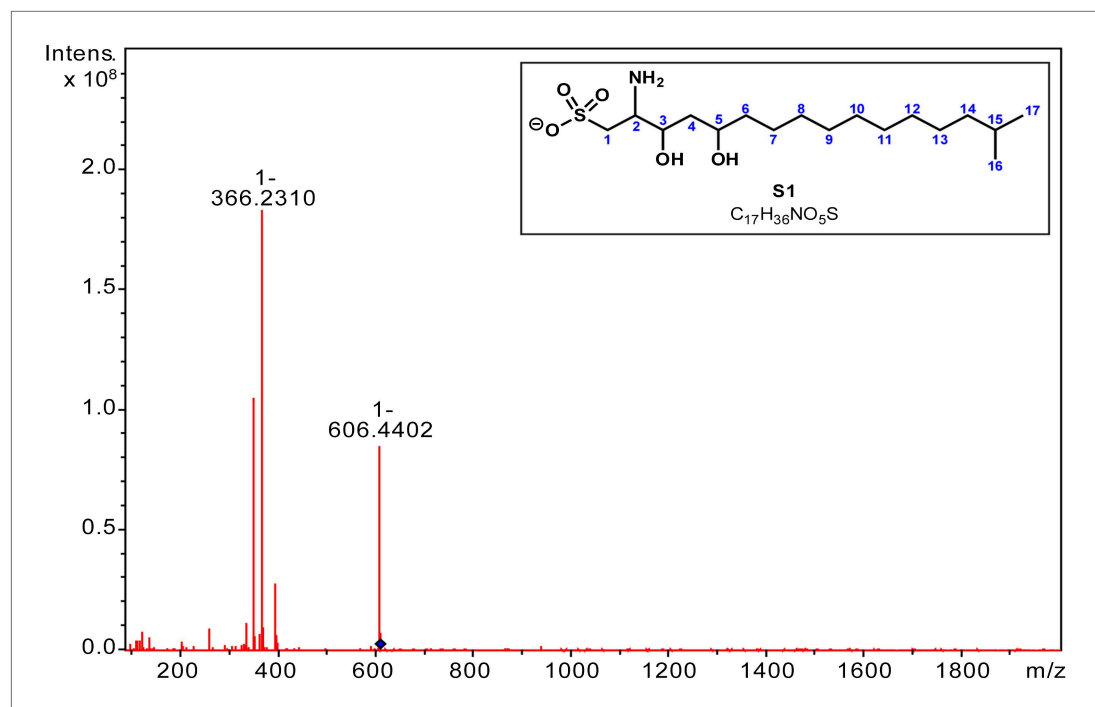
**Figure 3.** RIF-1, a sulfonolipid that induces rosette colony development. **(A)** Rosette colony development is induced by live *A. machiponganensis* and the sphingolipid-enriched lipid fraction (20 mg mL<sup>-1</sup>), but not by fresh medium, *A. machiponganensis* LPS (10 mg mL<sup>-1</sup>), PGN (50 mg mL<sup>-1</sup>), or LPS+PGN. Shown are the whisker-box plots of the % colonial cells/total cells under each condition in three independent experiments. **(B)** The molecular structure of RIF-1 deduced from MS and 1D- and 2D-NMR data. The RIF-1 structure, 3,5-dihydroxy-2-(2-hydroxy-13-methyltetradecanamido)-15-methylhexadecane-1-sulfonic acid, has two parts: a base (shown in red) that defines the capnoid, and a fatty acid (shown in black). Features that distinguish RIF-1 from other known capnoids are shown with colored arrows: the 2-hydroxy on the fatty acid (black) and the 5-hydroxy on the capnoid base (red).

DOI: 10.7554/eLife.00013.008



**Figure 3—figure supplement 1.** Separation of *A. machiponganensis* sphingolipids by thin layer chromatography (TLC). Lipids enriched in sphingolipids were separated by TLC after visualization with ammonium molybdate in 10%  $H_2SO_4$ . Bands (1-12) as well as regions between bands (A-F) were tested for morphogenic activity. Region F possessed activity and was further purified.

DOI: 10.7554/eLife.00013.009



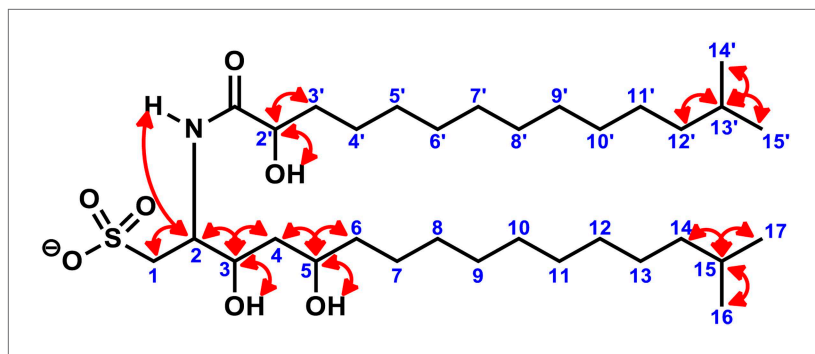


**Figure 3—figure supplement 3.** Key two-dimensional (2D) correlations of RIF-1: Observed COSY correlations. Red double-head arrows show key  $^3$ J or  $^4$ J H-H correlations in the head regions (1 to 6 and 2' to 3') of the fatty acid and the capnine base and in the tail regions with geminal dimethyl groups (14 to 17 and 12' to 15').

DOI: 10.7554/eLife.00013.011

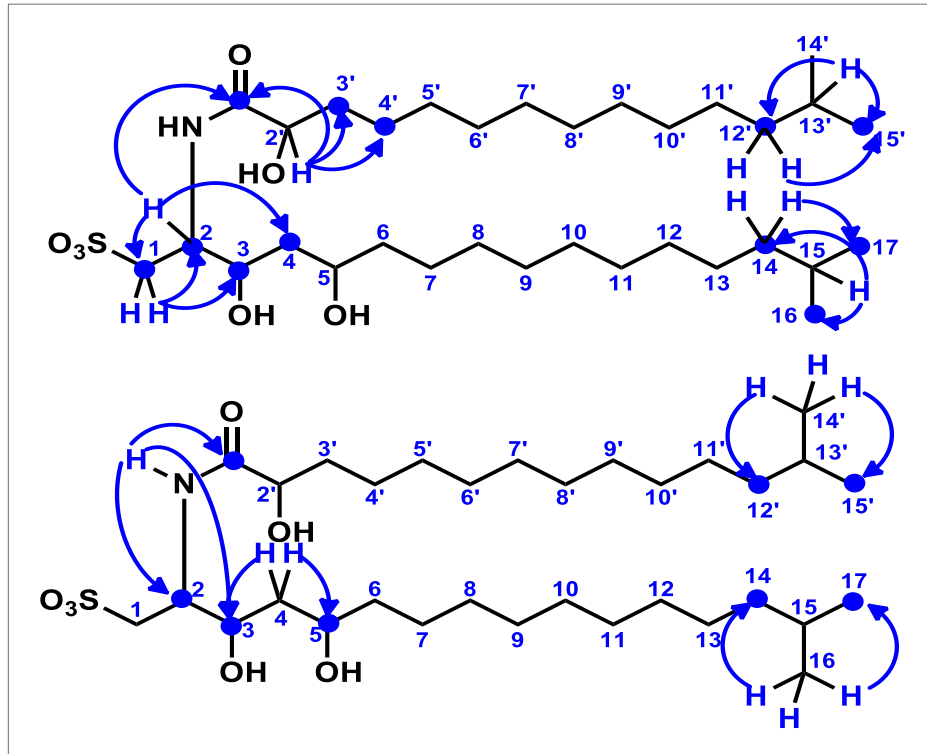


**Figure 3—figure supplement 4.** Key two-dimensional (2D) correlations of RIF-1: Observed HMBC spin system. Blue single-head arrows show key  $^2$ J or  $^3$ J H-C correlations in the head and tail regions of the fatty acid and capnine base. The correlations between C-1' and H-2/N-H demonstrated that the fatty acid and capnine base are joined through an amide bond.

DOI: 10.7554/eLife.00013.012

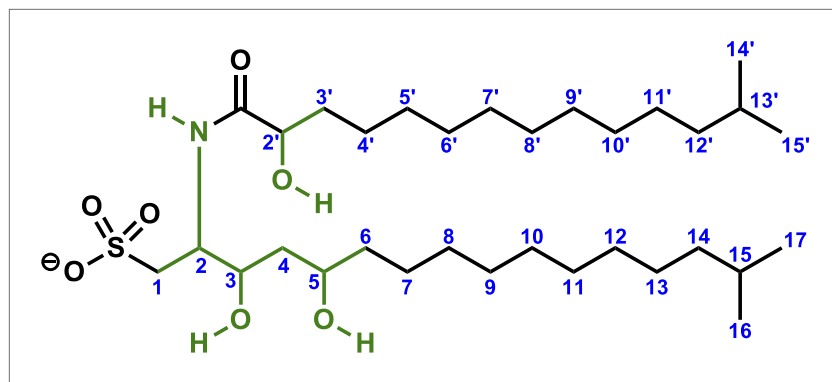


**Figure 3—figure supplement 5.** Key two-dimensional (2D) correlations of RIF-1: Observed TOCSY spin system. Green bonds show two key spin systems in RIF-1 - HO-CH- in the fatty acid fragment and -CH<sub>2</sub>-CH(NH)-CH(OH)-CH<sub>2</sub>-CH(OH)-CH<sub>2</sub>- in the capnene base fragment.

DOI: 10.7554/eLife.00013.013

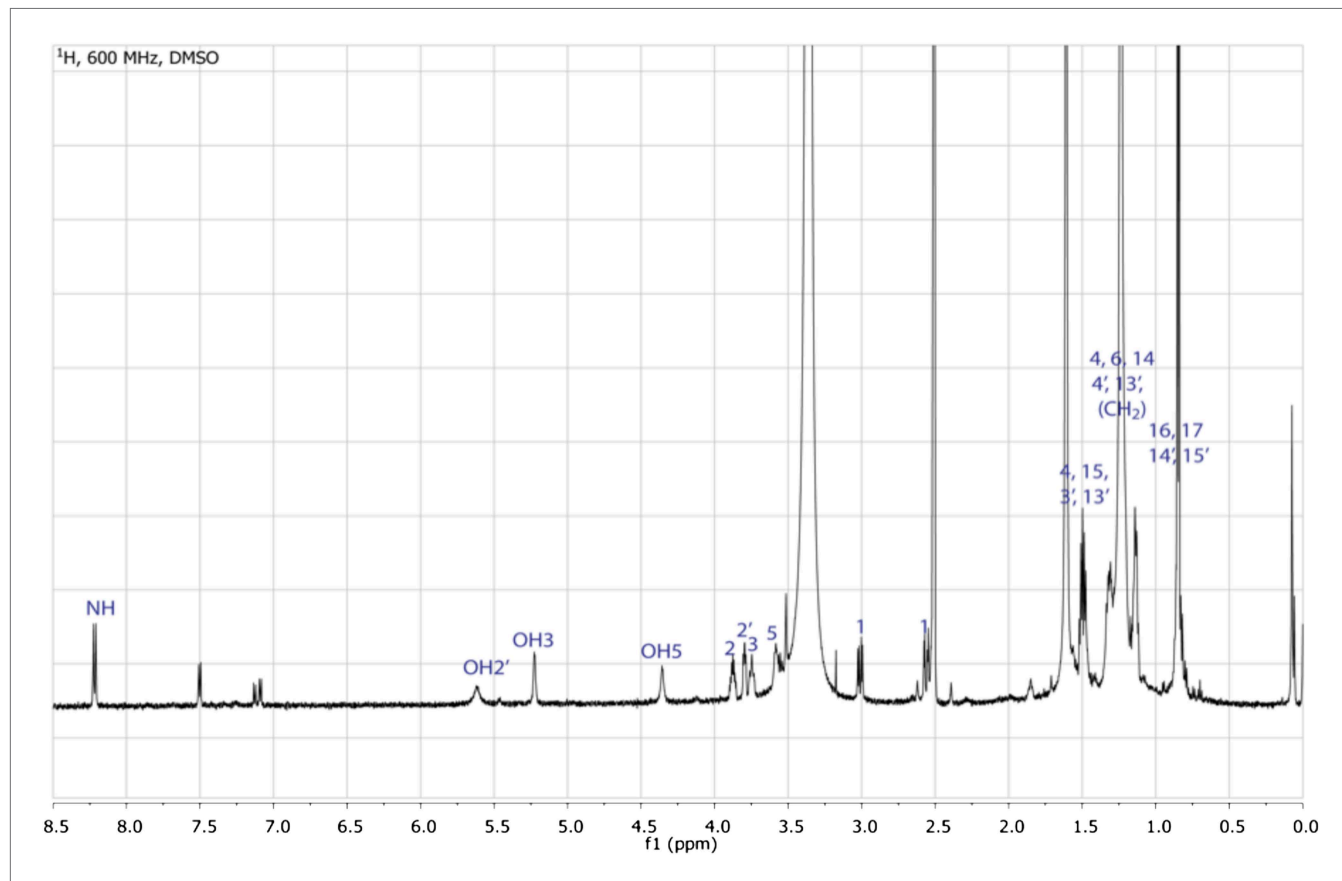


**Figure 3—figure supplement 6.** <sup>1</sup>H NMR spectrum of RIF-1. The spectrum exhibits one NH ( $\delta_{\text{H}}$  8.21), three hydroxyl groups ( $\delta_{\text{H}}$  5.52, 5.20, and 4.31), five signals from 2.50-4.00 ppm (four methines connected to either nitrogen at  $\delta_{\text{H}_2}$  3.88 or oxygens at  $\delta_{\text{H}_2'}$  3.80/ $\delta_{\text{H}_3}$  3.71-3.78/ $\delta_{\text{H}_5}$  3.53-3.61, and one methylene connected to sulfur at  $\delta_{\text{H}_1}$  2.56 & 3.01), twenty methylenes and four methyls ( $\delta_{\text{H}}$  d,  $J = 6.6$  Hz, 12H) in the high field region ( $\delta_{\text{H}}$  0.75-1.75 ppm).

DOI: 10.7554/eLife.00013.014

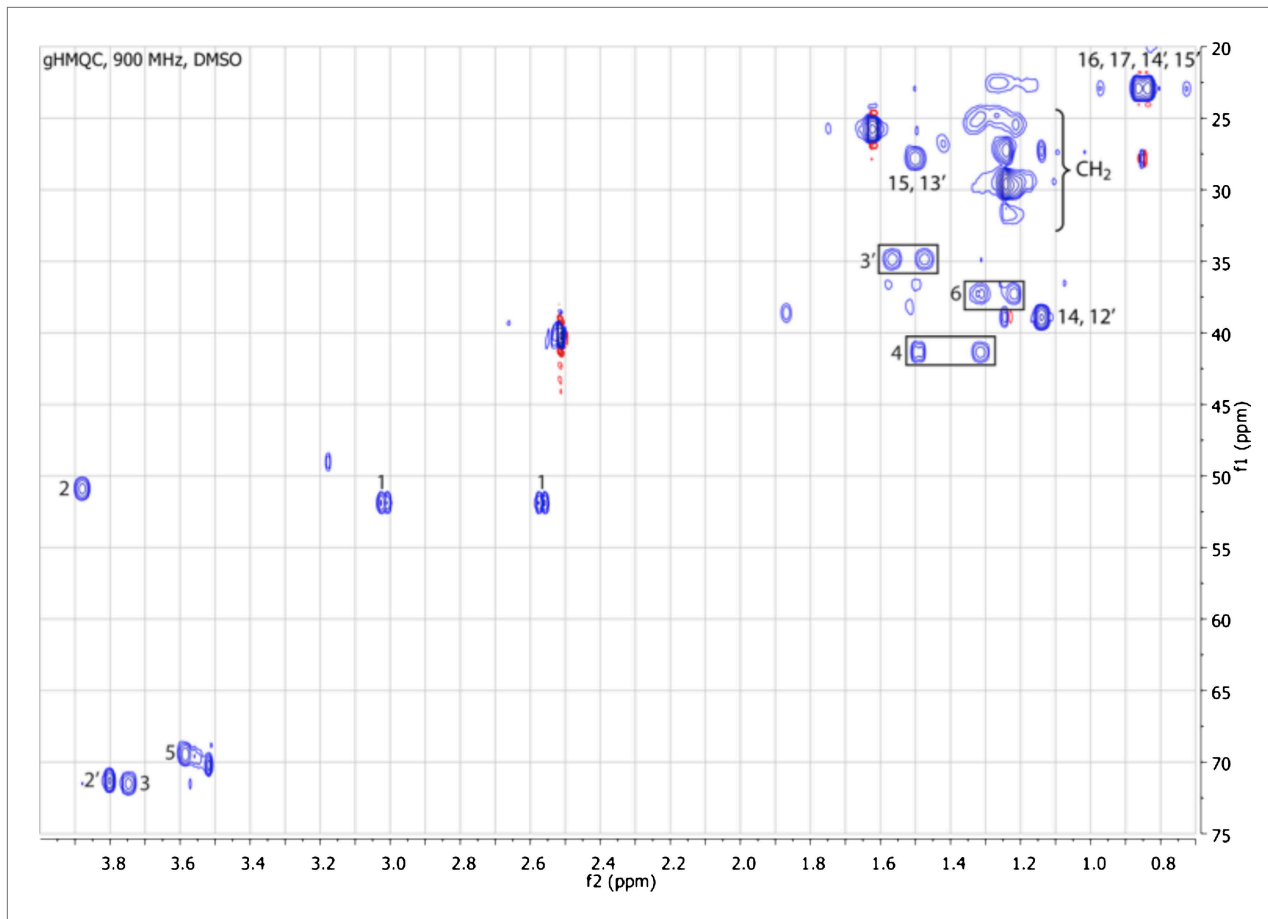


**Figure 3—figure supplement 7.** gHMQC spectrum of RIF-1. The  $^1\text{J}$  H-C correlations demonstrate that  $2(\delta_{\text{H}} 3.88, \delta_{\text{C}} 50.89)$  is connected to a nitrogen;  $2', 3,$  and  $5(\delta_{\text{H}} 3.80/\delta_{\text{C}} 71.29, \delta_{\text{H}} 3.71\text{--}3.78/\delta_{\text{C}} 71.51,$  and  $\delta_{\text{H}} 3.53\text{--}3.61/\delta_{\text{C}} 70.20,$  respectively) are oxygenated;  $1(\delta_{\text{H}} 3.01$  and  $2.56, \delta_{\text{C}} 51.87)$  is adjacent to a sulfonic acid group; and all the other twenty methylenes and four methyls at high filed ( $\delta_{\text{H}} 0.75\text{--}1.75/\delta_{\text{C}} 22.00\text{--}42.00$ ).

DOI: 10.7554/eLife.00013.015

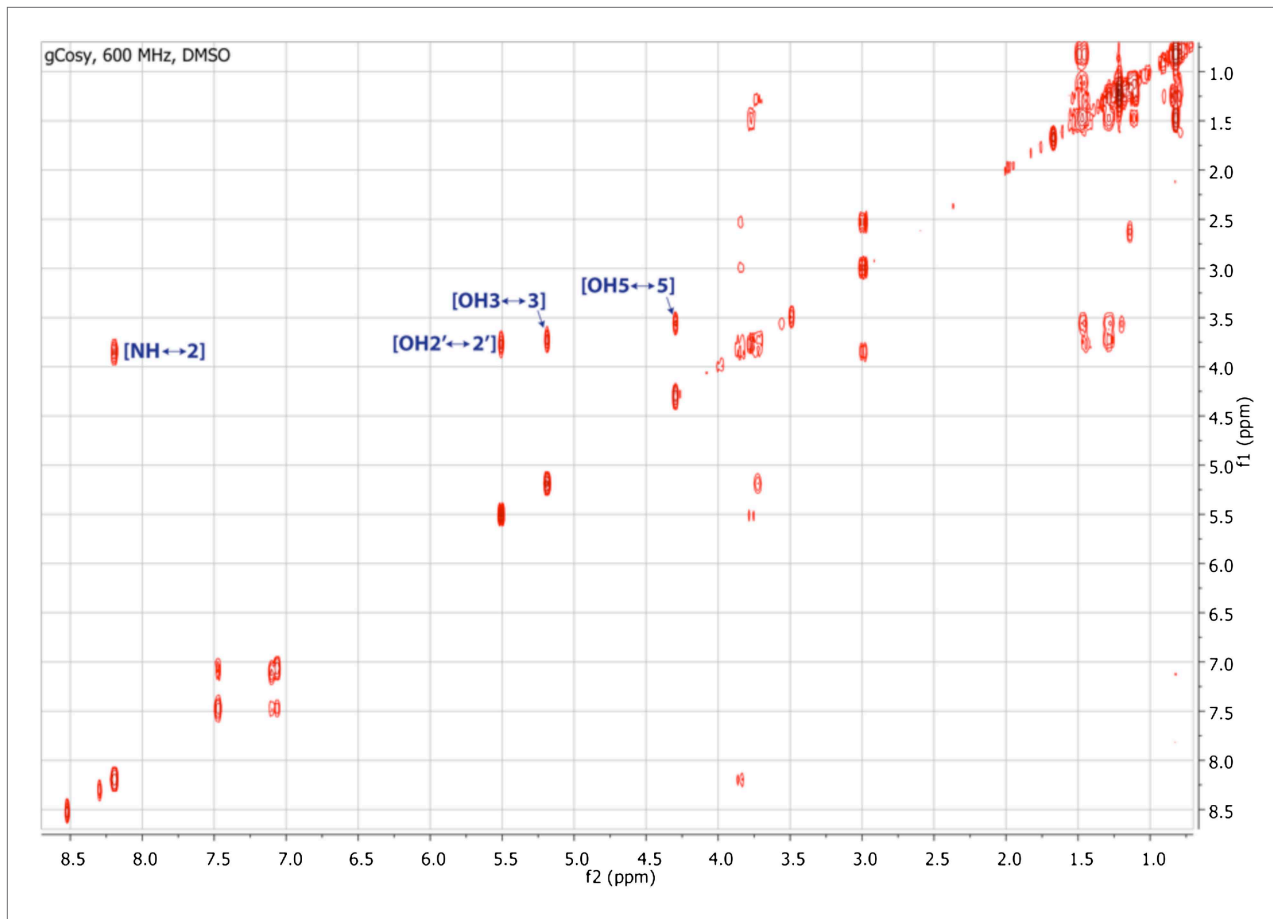


**Figure 3—figure supplement 8.** gCOSY spectrum of RIF-1. Indicated are important H-H correlations between NH and H-2', 2'-OH and H-2', 3-OH and H-3, and 5-OH and H-5.

DOI: 10.7554/eLife.00013.016

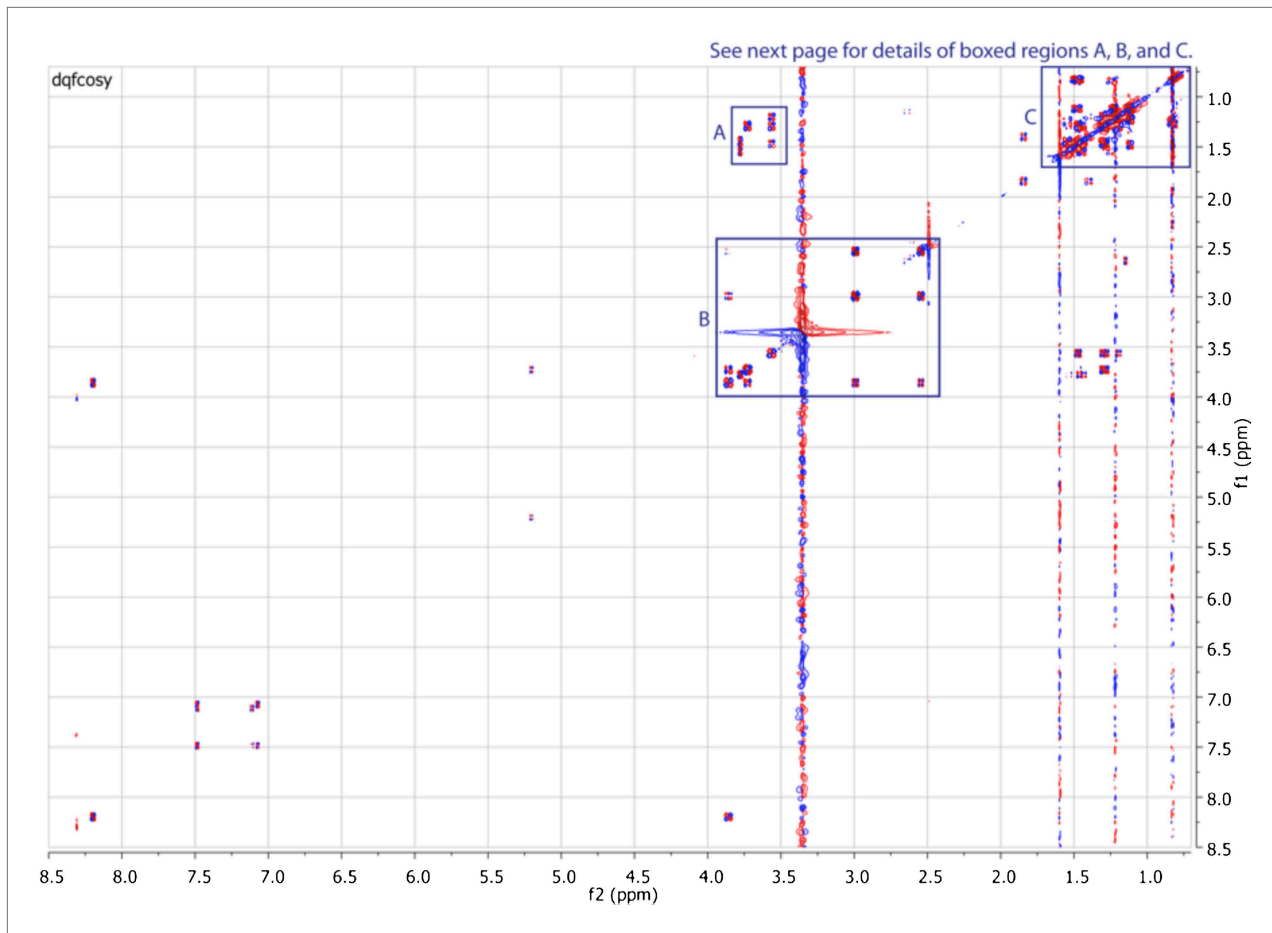


**Figure 3—figure supplement 9.** Expanded dqcOSY spectrum of RIF-1. In panel A ( $\delta_H$  1.15-1.65 ppm/ $\delta_H$  3.52-3.82 ppm), H-3 ( $\delta_H$  3.73) shows correlation to H-4a ( $\delta_H$  1.30), H-5 ( $\delta_H$  3.57) to H-4a/H-4b ( $\delta_H$  1.30/1.47), and H-5 to H<sub>2</sub>-6 ( $\delta_H$  1.20/1.29); H-2' ( $\sim\delta_H$  3.8) correlates to H<sub>2</sub>-3' ( $\delta_H$  1.45 and 1.54). Panel B ( $\delta_H$  2.4-4.0 ppm/ $\delta_H$  2.4-4.0 ppm) demonstrates the correlations between H<sub>2</sub>-1 ( $\delta_H$  2.56/ $\sim$ 3.0) and H-2 ( $\delta_H$  3.88), and between H-2 and H-3. Panel C ( $\delta_H$  0.75-1.60 ppm/ $\delta_H$  0.75-1.60 ppm) exhibits correlations in the other methylenes and methyl groups.

DOI: 10.7554/eLife.00013.017

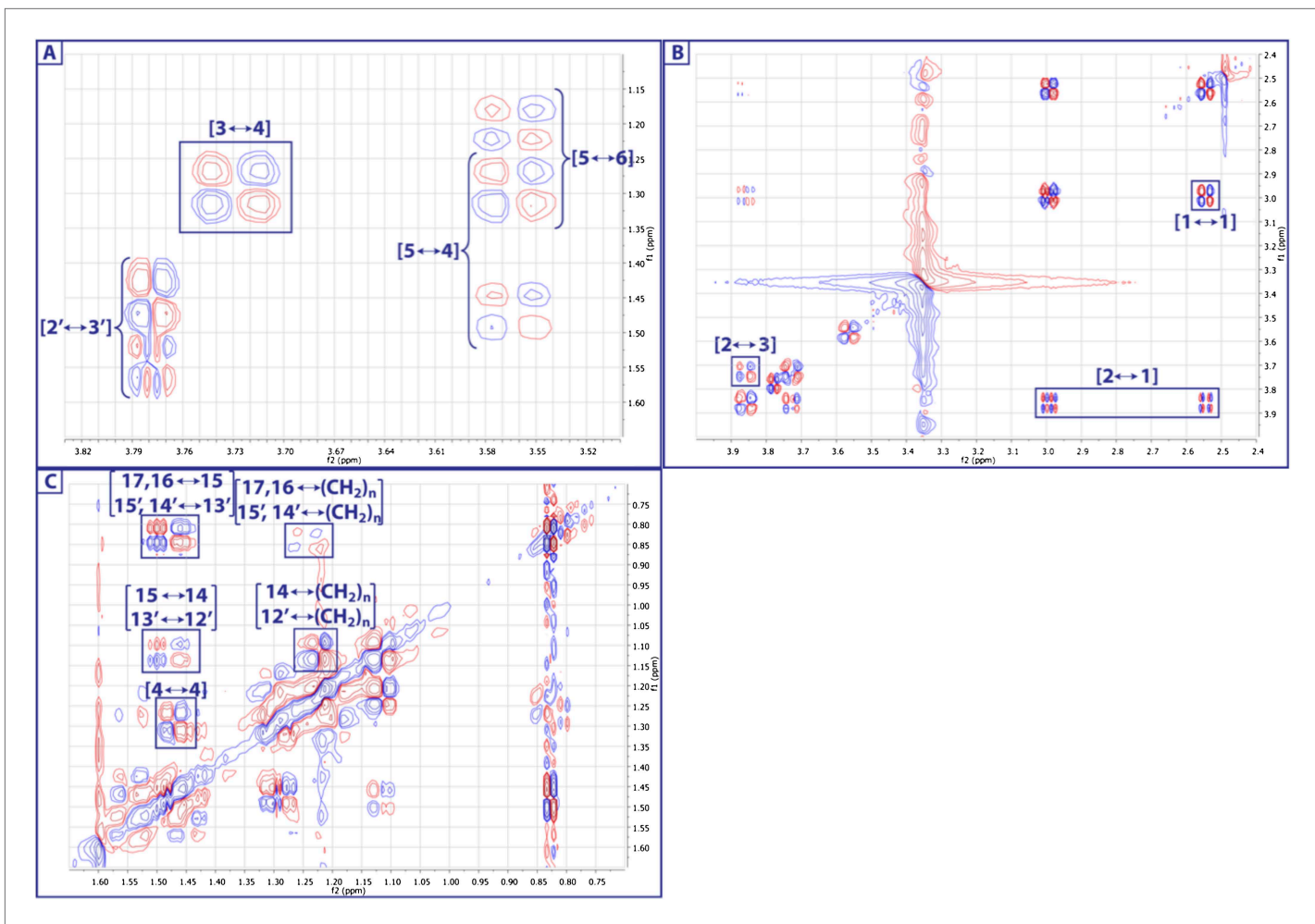


**Figure 3—figure supplement 10.** Expanded dqfCOSY spectra of RIF-1. A dqfCOSY spectrum was collected in order to get a clear connectivity in the oxygenated region (1-position to 6-position) in the capnoid base fragment.

DOI: 10.7554/eLife.00013.018

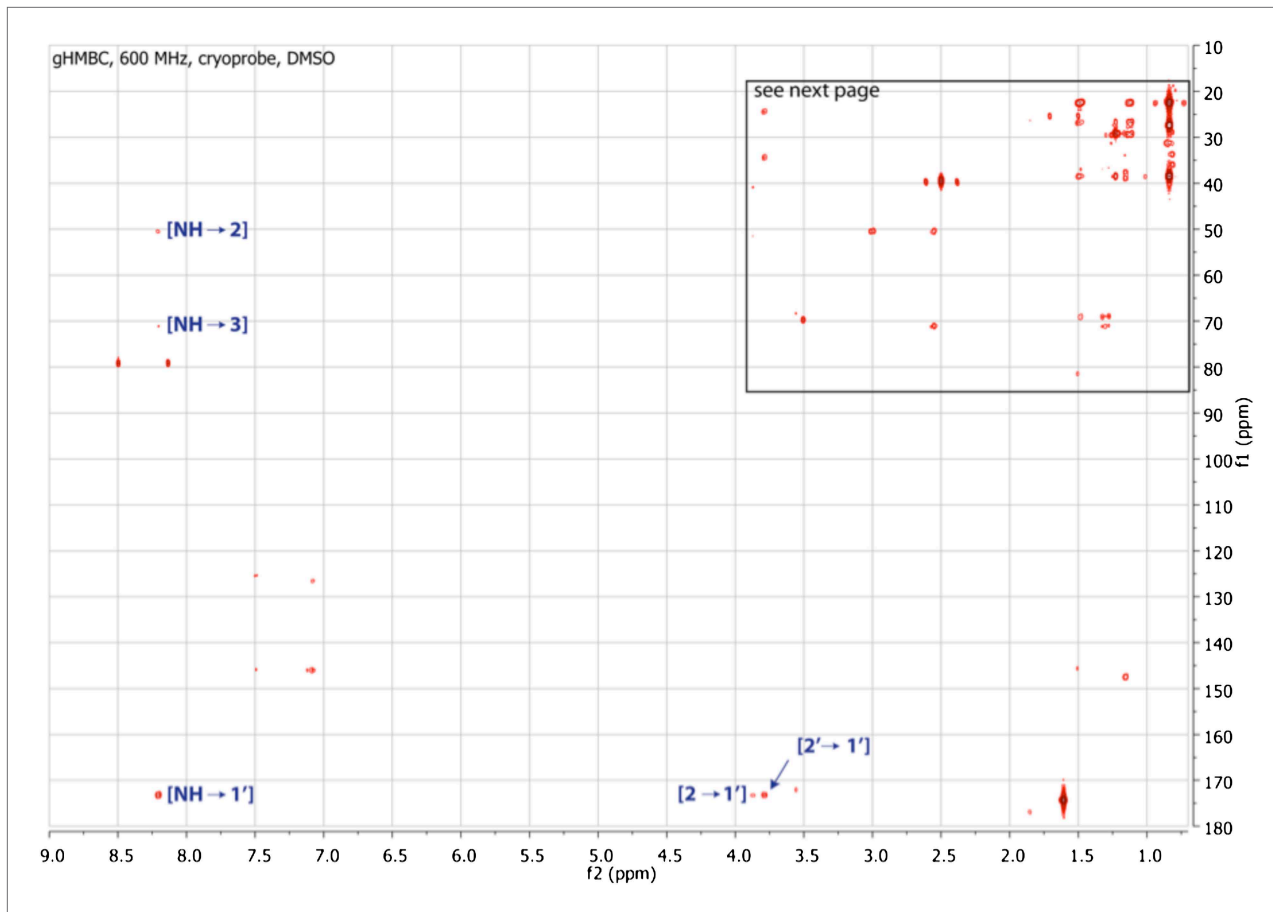


**Figure 3—figure supplement 11.** gHMBC spectrum of RIF-1. Indicated are important  $^2$ J or  $^3$ J H-C correlations between NH/H-2/H-2' and C-1' ( $\delta_c$  173.23), and between NH and C-2/C-3 ( $\delta_c$  50.89/71.51). Based on the MS/MS analysis, the fatty acid fragment must be 2-hydroxy-13-methyltetradecanoyl, and the capnine base fragment must be 2-NH-3,5-dihydroxy-15-methylhexadecane-1-sulfonate. Hence, the planar structure of RIF-1 is determined as shown in **Fig. 3** and **Fig. 3 – Figure Supplements 3-5**.

DOI: 10.7554/eLife.00013.019

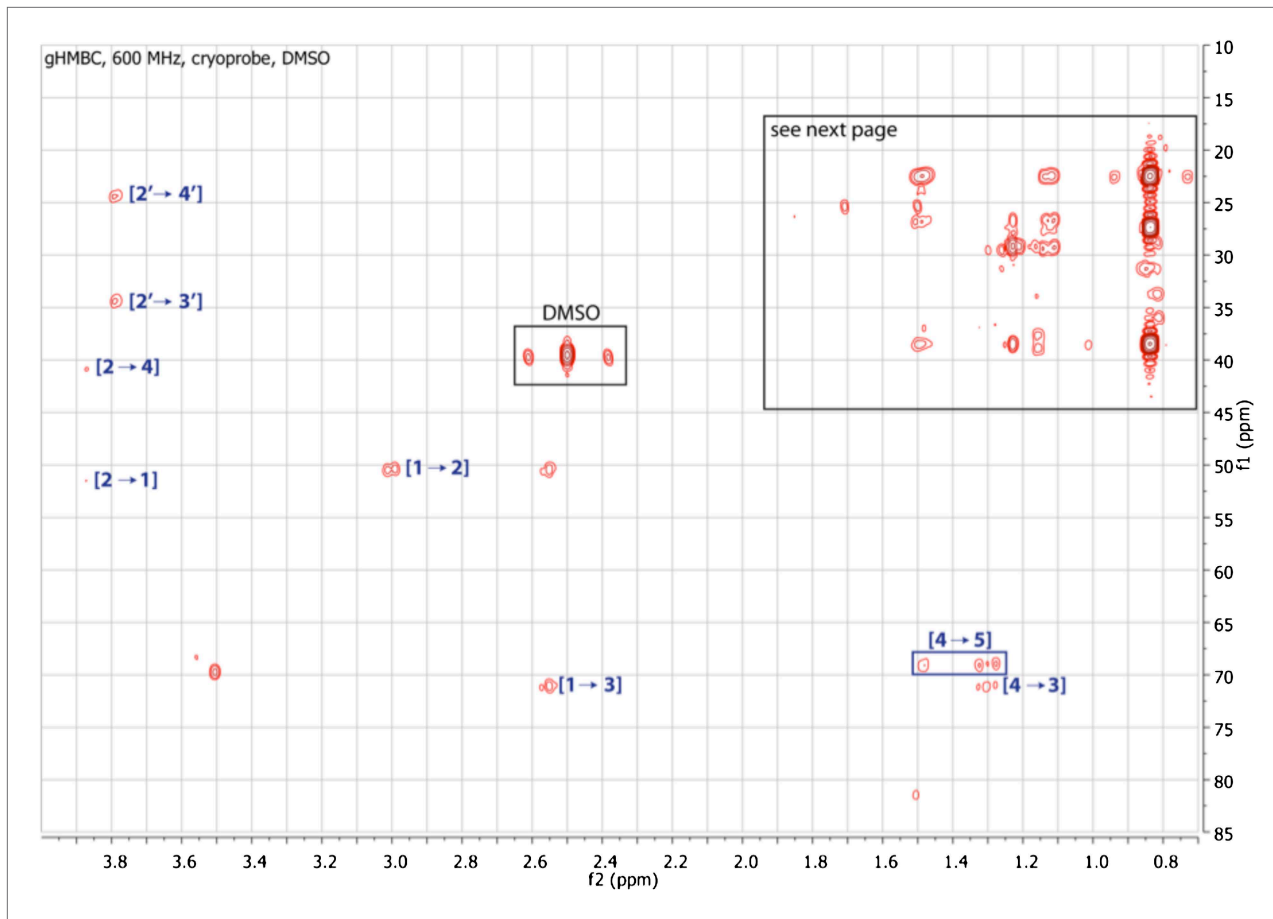


**Figure 3—figure supplement 12.** Expanded gHMBC spectrum of RIF-1 ( $\delta_{\text{H}}$  0-4.00 ppm/ $\delta_{\text{C}}$  15.0-85.0 ppm). Indicated are correlations between H-2 to C-4/C-1 ( $\delta_{\text{C}}$  41.36/51.87), between H-2' and C-4'/C-3' ( $\delta_{\text{C}}$  24.99/34.85), between H-1 and C-2/C-3 ( $\delta_{\text{C}}$  50.89/71.51), and between H-4 and C-5/C-3 ( $\delta_{\text{C}}$  70.20/71.51).

DOI: 10.7554/eLife.00013.020

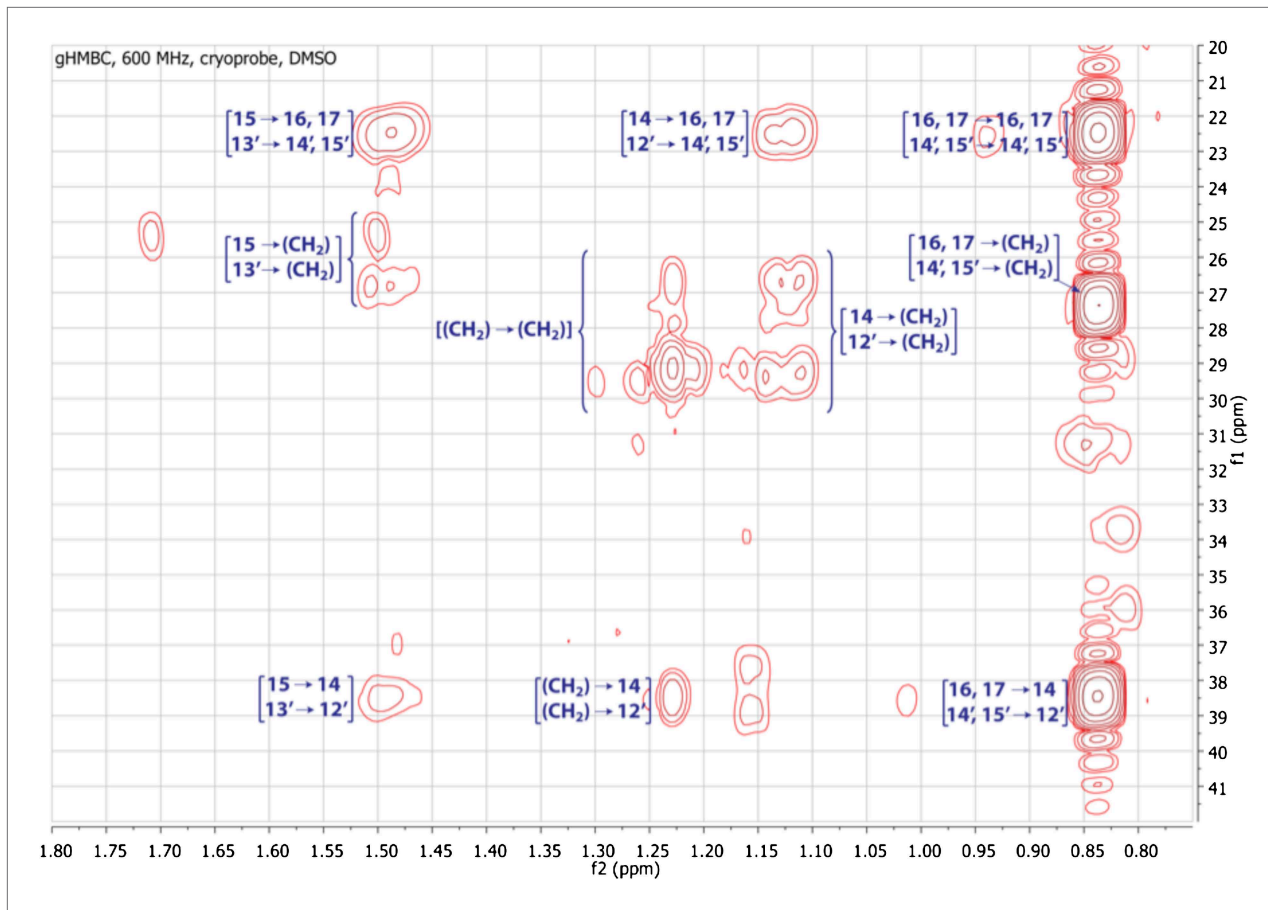


**Figure 3—figure supplement 13.** Expanded gHMBC spectrum of RIF-1 ( $\delta_H$  0.80-1.80 ppm/ $\delta_C$  20.0-40.0 ppm). Key correlations are between H-16 and C-14/C-15/C-17 ( $\delta_C$  38.91/27.79/22.09), between H-17 and C-14/C-15/C-16 ( $\delta_C$  38.91/27.79/22.09), between H-14' and C-12'/C-13'/C-15' ( $\delta_C$  38.91/27.79/22.09), and between H-15' and C-12'/C-13'/C-14' ( $\delta_C$  38.91/27.79/22.09).

DOI: 10.7554/eLife.00013.021

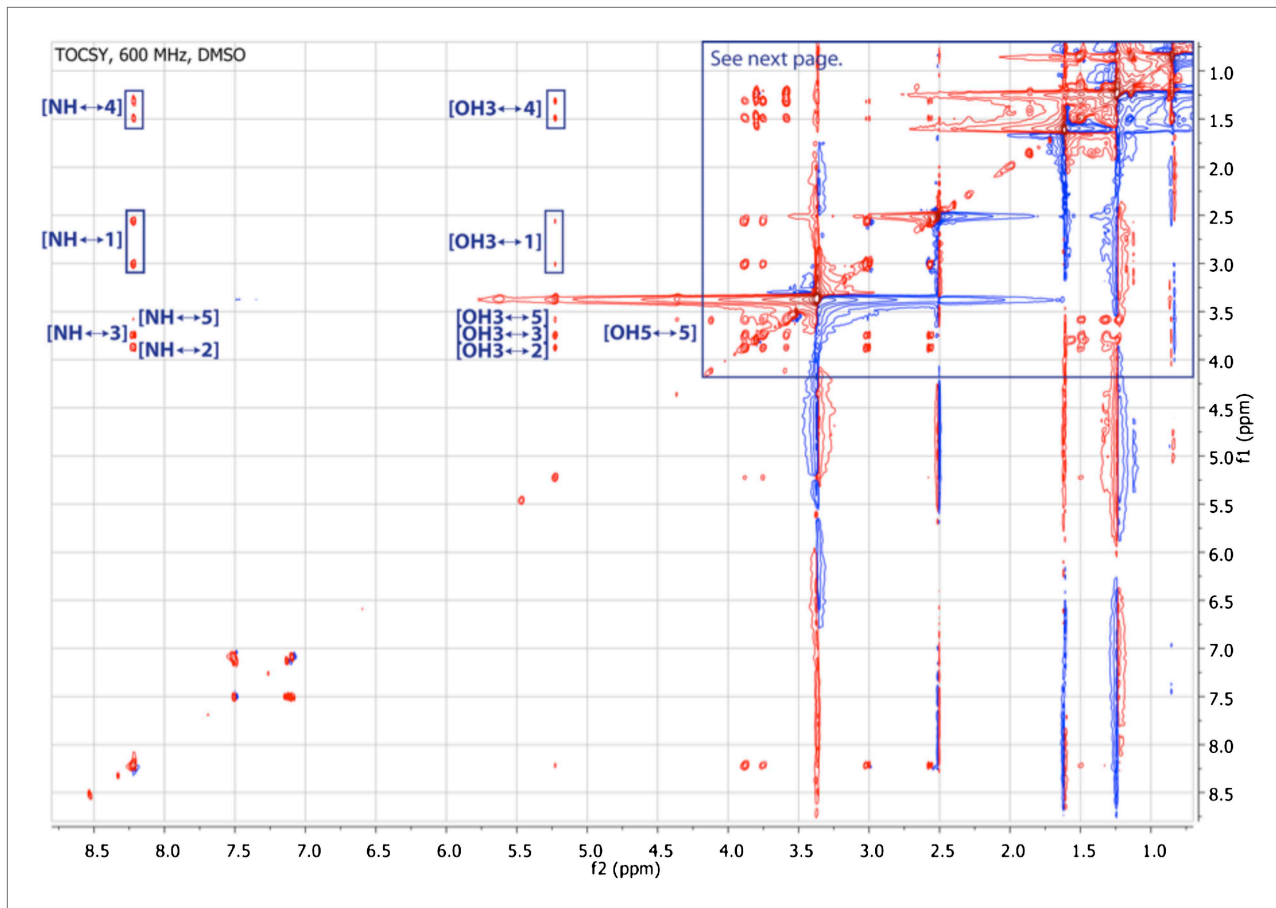


**Figure 3—figure supplement 14.** TOCSY spectrum of RIF-1. The spectrum shows correlations from NH to H-1 and H-5 through H-2, H-3 and H-4, and from 3-OH to H-5 via H-4 and H-1 through H-3 and H-2.

DOI: 10.7554/eLife.00013.022

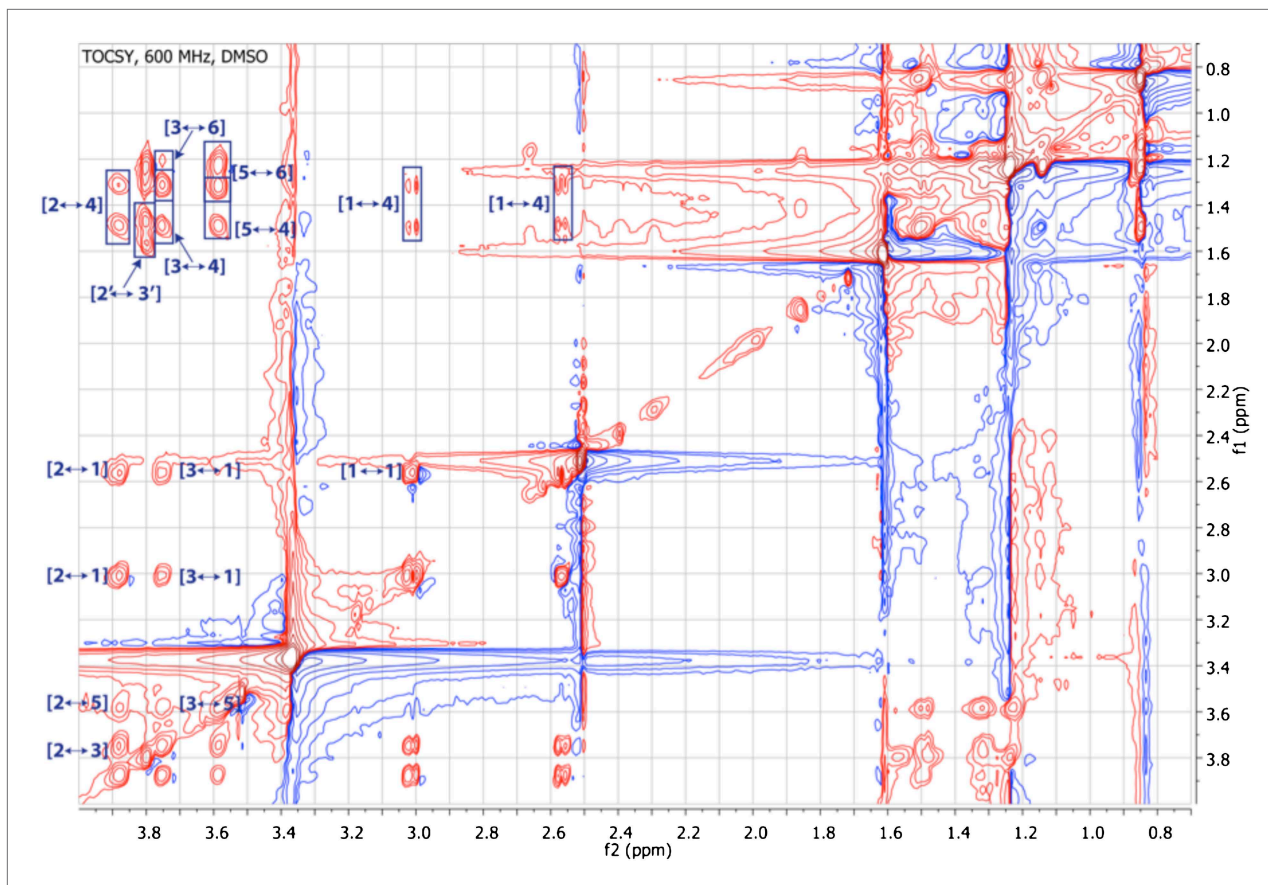


**Figure 3—figure supplement 15.** Expanded TOCSY spectrum of RIF-1 ( $\delta_H$  0.50-4.25 ppm/ $\delta_C$  0.50-4.25 ppm). Another important spin system is clearly demonstrated by the TOCSY correlations between H-2' and H<sub>2</sub>-3'/H-4'/H-5' on the top left of the expanded spectrum.

DOI: 10.7554/eLife.00013.023

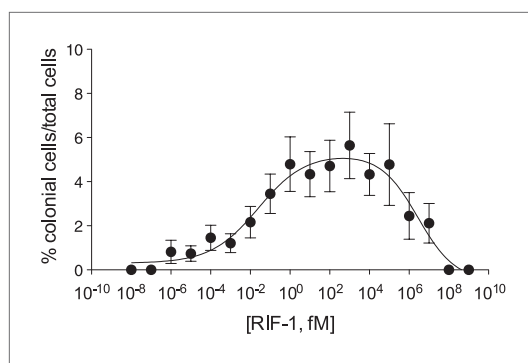


**Figure 4.** Purified RIF-1 is active at plausible environmental concentrations. RIF-1 concentrations ranging from  $10^{-2}$  to  $10^7$  fM induce rosette colony development in RCA cultures. Frequency of rosette colony development was quantified in RCA cultures 2 days after treatment with a dilution series of purified RIF-1. Data are mean  $\pm$  s.e. from three independent experiments. Line indicates non-linear regression of the RIF-1 activity profile.

DOI: 10.7554/eLife.00013.025

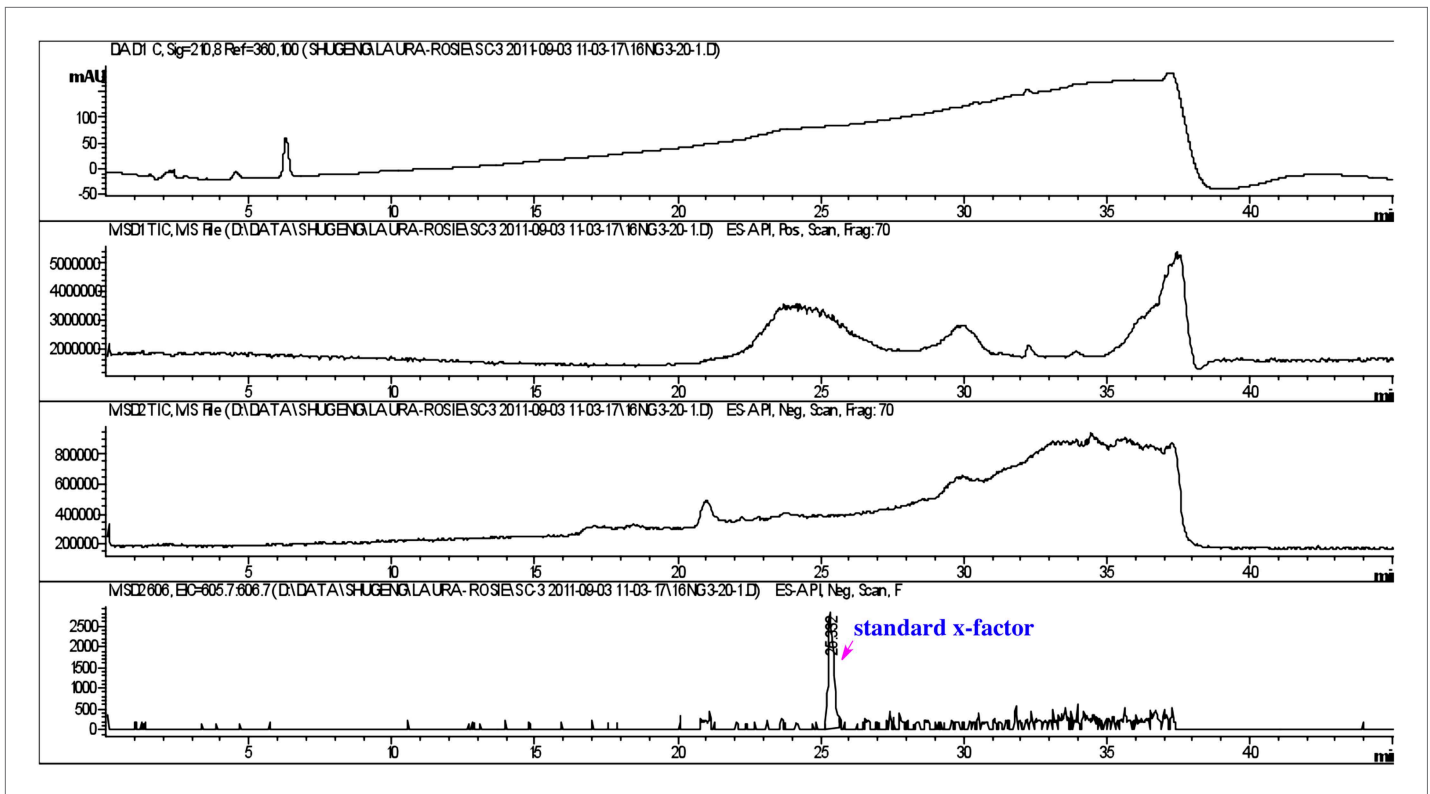


**Figure 4—figure supplement 1.** Detection of purified RIF-1. RIF-1 did not show absorbance at 210 nm (top panel), but the molecule (606 Da, M-H<sup>+</sup>) was detected between 25 and 26 minutes (bottom panel).

DOI: 10.7554/eLife.00013.026

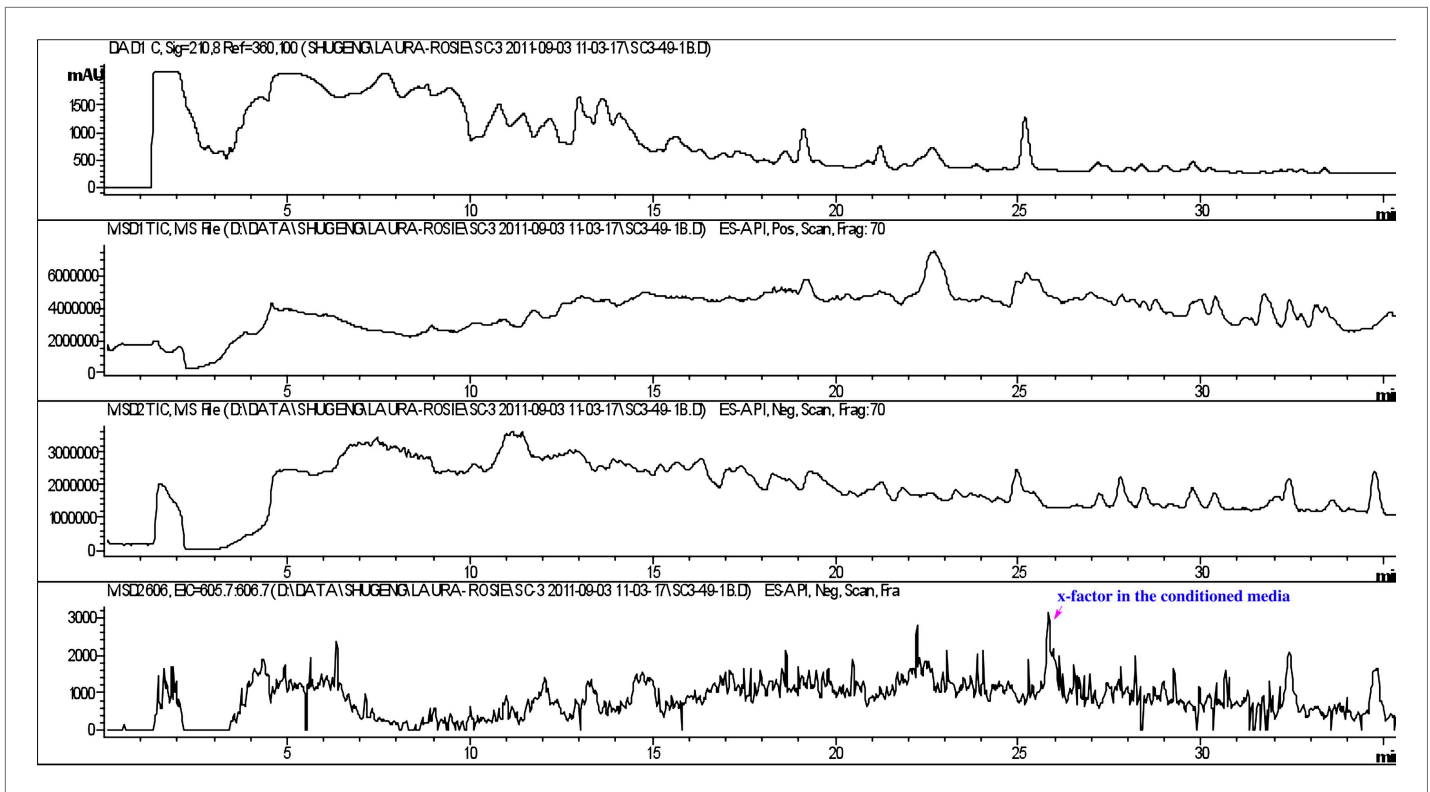


**Figure 4—figure supplement 2.** Detection of RIF-1 in the conditioned medium of *A. machipongonensis*. RIF-1 (bottom panel) was detected in the conditioned medium after the broth was concentrated 250 times.

DOI: 10.7554/eLife.00013.027

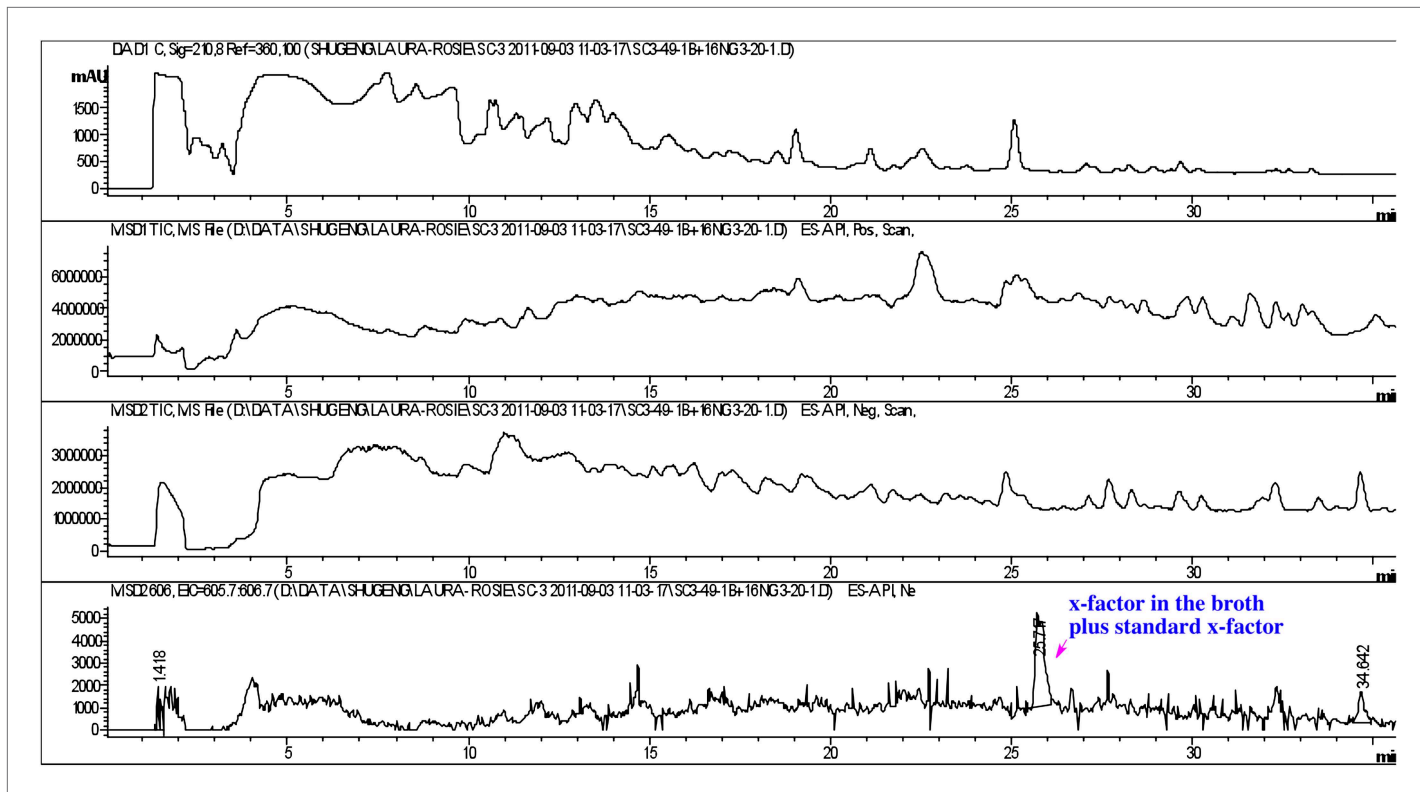


**Figure 4—figure supplement 3.** Co-injection of concentrated conditioned medium with purified RIF-1. The peak of the RIF-1 in the conditioned medium was enhanced after the sample was spiked with purified RIF-1 (bottom panel).

DOI: 10.7554/eLife.00013.028